Biomedicine & Pharmacotherapy 174 (2024) 116466

Contents lists available at ScienceDirect

Biomedicine & Pharmacotherapy

journal homepage: www.elsevier.com/locate/biopha

Hydrogen sulfide dysfunction in metabolic syndrome-associated vascular complications involves cGMP regulation through soluble guanylyl cyclase persulfidation

M. Smimmo [a], V. Casale [a], G.M. Casillo [a], E. Mitidieri [a], R. d'Emmanuele di Villa Bianca [a], I. Bello [a], A. Schettino [a], R. Montanaro [b], V. Brancaleone [b], C. Indolfi [c], G. Cirino [a], A. Di Lorenzo [d], M. Bucci [a,*], E. Panza [a,1], V. Vellecco [a,1]

[a] Department of Pharmacy, School of Medicine and Surgery, University of Naples Federico II, Naples, Italy
[b] Department of Science, University of Basilicata, Potenza, Italy
[c] Department of Molecular Medicine and Medical Biotechnology, School of Medicine and Surgery, University of Naples Federico II, Naples 80131, Italy
[d] Department of Pathology and Laboratory Medicine Center for Vascular Biology, Weill Cornell Medical College, Cornell University, New York, USA

ARTICLE INFO

Keywords:
H_2S donors
aorta
db/db mice
soluble guanylyl cyclase
metabolic syndrome

ABSTRACT

Here, by using *in vitro* and *ex vivo* approaches, we elucidate the impairment of the hydrogen sulfide (H_2S) pathway in vascular complications associated with metabolic syndrome (MetS). In the *in vitro* model simulating hyperlipidemic/hyperglycemic conditions, we observe significant hallmarks of endothelial dysfunction, including eNOS/NO signaling impairment, ROS overproduction, and a reduction in CSE-derived H_2S. Transitioning to an *ex vivo* model using db/db mice, a genetic MetS model, we identify a downregulation of CBS and CSE expression in aorta, coupled with a diminished L-cysteine-induced vasorelaxation. Molecular mechanisms of eNOS/NO signaling impairment, dissected using pharmacological and molecular approaches, indicate an altered eNOS/Cav-1 ratio, along with reduced Ach- and Iso-induced vasorelaxation and increased L-NIO-induced contraction. *In vivo* treatment with the H_2S donor Erucin ameliorates vascular dysfunction observed in db/db mice without impacting eNOS, further highlighting a specific action on smooth muscle component rather than the endothelium. Analyzing the NO signaling pathway in db/db mice aortas, reduced cGMP levels were detected, implicating a defective sGC/cGMP signaling. *In vivo* Erucin administration restores cGMP content. This beneficial effect involves an increased sGC activity, due to enzyme persulfidation observed in sGC overexpressed cells, coupled with PDE5 inhibition. In conclusion, our study demonstrates a pivotal role of reduced cGMP levels in impaired vasorelaxation in a murine model of MetS involving an impairment of both H_2S and NO signaling. Exogenous H_2S supplementation through Erucin represents a promising alternative in MetS therapy, targeting smooth muscle cells and supporting the importance of lifestyle and nutrition in managing MetS.

1. Introduction

Metabolic syndrome (MetS) is a cluster of metabolic abnormalities that are associated with visceral adiposity. These disorders include insulin resistance, hyperglycemia, hypertension, and dyslipidemia (low high-density lipoprotein cholesterol, and hypertriglyceridemia). According to the International Diabetes Foundation, this syndrome is diagnosed by the co-occurrence of three of the five metabolic abnormalities and it is strongly associated with an increased risk of developing type 2 diabetes and atherosclerotic and nonatherosclerotic cardiovascular disease (CVD) [1]. In recent times, the exponential increase in obesity has remarkably increased the incidence of MetS (https://www.

Abbreviations: 3-MST, 3-mercaptopyruvate sulfurtransferase; CBS, cystathionine- β-synthase; CSE, cystathionine-γ-lyase; DPD, N,N-dimethyl-p-phenylenediamine; eNOS, endothelial nitric oxide synthase; ETHE-1, ethylmalonic encephalopathy 1 protein; $FeCl_3$, iron chloride; H_2S, hydrogen sulfide; L-NIO, N5-1-Iminoethyl-L-ornithine dihydrochloride; MetS, metabolic syndrome; NO, nitric oxide; NO^{2-}, nitrite; NO^{3-}, inorganic anion nitrate; PDE, phosphodiesterase; sGC, soluble guanilyl cyclase; SQRLD, sulfide quinone reductase; cGMP, cyclic guanosine-monophosphate; Cav-1, caveolin-1; ROS, radical oxygen species.

* Correspondence to: Department of Pharmacy, School of Medicine and Surgery, University of Naples Federico II, via D. Montesano 49, Naples 80131, Italy.
E-mail address: mrbucci@unina.it (M. Bucci).

[1] the authors share the last authorship

https://doi.org/10.1016/j.biopha.2024.116466
Received 22 December 2023; Received in revised form 14 March 2024; Accepted 15 March 2024
Available online 28 March 2024

who.int/news/item/04–03-2022-world-obesity-day-2022-accelerating-action-to-stop-obesity). The first approach in MetS treatment is lifestyle changes with exercise and diet to induce weight loss, followed by drug therapy aimed at treating atherogenic dyslipidemia, hypertension, and hyperglycemia.

Vascular inflammation is one of the main recognized clinical manifestations of MetS, where endothelium dysfunction represents the first event that occurs in the vascular wall. It is characterized by an overproduction of free radical oxygen species (ROS) coupled with impairment of endothelial nitric oxide synthase/nitric oxide (eNOS/NO) signaling (defined as eNOS uncoupling), with the consequent reduction in vasodilating properties, pro-coagulability, and arterial stiffness [2]. In this complex scenario, a role for transsulfuration pathway (TSP), and specifically for hydrogen sulfide (H_2S) signaling, is emerging. H_2S is a gasotransmitter endogenously produced within the body by the reverse TSP [3,4]. The main enzymes responsible for H_2S biosynthesis are cystathionine-γ lyase (CSE), cystathionine-β synthase (CBS), and 3- mercaptopyruvate sulfurtransferase (3-MST).

These constitutive enzymes have distinct expression profiles and subcellular distributions: indeed, under physiological conditions, 3-MST is localized in both cytosol and mitochondria, while CSE and CBS are distributed mainly in the cytosol [3,4]. It is well known that CSE is the major source of H_2S in the cardiovascular system contributing to vascular homeostasis inducing vasorelaxation, improving endothelial dysfunction, and attenuating atherosclerotic plaque formation [5–9]. The relevance of H_2S signaling within the vasculature is demonstrated by the finding that plasmatic levels of H_2S are significantly reduced in diabetes and hypertension, in human and animal models [10–12]. Moreover, in rat aortic endothelial cells treated with high concentrations of glucose and palmitate, there is a reduction of both CSE expression and H_2S production, coupled with an increase in ROS production and mitochondrial apoptosis [13]. Here, by using *in vitro* and *ex vivo* approaches we demonstrate that i) an impairment of H_2S pathway is involved in vascular complications associated with MetS; ii) an *in vivo* treatment with an H_2S donor Erucin, can rescue vascular complications; iii) the mechanism underlying this effect involves sGC persulfidation leading to an increased cGMP production.

2. Methods

2.1. Animal model and drug treatment

Animal care and experimental procedures in this study follow specific guidelines of the Italian and European Council law for experiments involving animals. All procedures were approved by the local animal care office (Centro Servizi Veterinari, University of Naples, Federico II) and carried out following ARRIVE guidelines [14] and EU recommendations (Directive 2010/63/EU) for experimental design and analysis in pharmacology care. The procedure was authorized by Ministero della Salute (prot. n. 97/2020). For this study, male db/db mice or their lean db/+ littermates of 5 weeks of age were purchased from Charles River Laboratories (MI, Italy) and were housed in the animal care facility at the Department of Molecular Medicine and Medical Biotechnology, School of Medicine and Surgery, University of Naples, Italy. All mice were housed in pathogen-free cages (three mice per cage) with a 12 h light-dark cycle (temperature 23 ± 2 °C, humidity 60%) and free access to dry feed and water. The evaluation of body weight and glycemia was performed weekly starting from 6 to 10 weeks of age, to monitor the onset and progression of MetS (see Table 1). Erucin (3 mg/Kg) or vehicle (potassium phosphate buffer pH 7.4) was administered orally by *gavage* to mice once a day for four weeks (from 6 to 10 weeks). The volume administered to each mouse was 100 μl/day. Animals were randomly assigned to the different experimental groups that included at least five mice.

2.2. Ex vivo isolated organ bath studies

Once at 10 weeks of age, db/db mice, treated with Erucin or vehicle, were anesthetized with enflurane (5%) and then killed in a CO_2 chamber (70%). The thoracic aorta was rapidly harvested, cleaned, cut and mounted in an isolated organ bath filled with oxygenated Krebs solution at 37°C, and connected to isometric transducers The rings were initially stretched until a resting tension of 1.0 g and equilibrated for at least 30 minutes [15,16]. In each set of experiments, rings were firstly challenged with PE (1 μM; cat. n. P6126; Merck, Milan, Italy) until the responses were reproducible. Then PE cumulative concentration-response curve was performed (1 nM–3 μM;). In a separate set of experiments, once a stable tone of PE (1 μM) was reached, a cumulative concentration-response curve of the following drugs was performed: Acetylcholine (Ach, 10 nM - 30 μM, cat. n. A9101; Merck, Milan, Italy), Isoprenaline (Iso, 10 nM-30 μM; cat. n. I5627; Merck, Milan, Italy), NaHS (10 nM −300 μM, Merck, 161527), Erucin (10 nM - 300 μM; cat. n. 14017; Cayman Chemical) and L-cysteine (10 nM −3 mM; cat. n. C1276Merck; Milan, Italy) were performed. In another set of experiments on phenylephrine-precontracted rings (300 nM), the contraction induced by N5-(1-Iminoethyl)-L-ornithine dihydrochloride (L-NIO; 10 μM cat. n. I134; Merck, Milan, Italy Merck), a selective inhibitor of eNOS was evaluated.

2.3. Cell culture experiments

2.3.1. Endothelial cells (BAEC) in high glucose and high palmitate environment

Bovine aortic endothelial cells (BAEC) were cultured and grown in medium (DMEM) supplemented with 2 mmol/L glutamine, 10% heat-inactivated fetal bovine serum, 50 U/ml penicillin/streptomycin. BAEC were incubated for 3 hours in 50 mM (high glucose) D-glucose (HG) solution plus 100 μM sodium palmitate (SP) solution to mimic hyperglycemic and hyperlipidemic (HG+SP) environment. Then cells were stimulated with insulin (100 nM, 15 min; cat. n. I6634; Merck, Milan, Italy). Following that time, pellets were collected and used for Western blot analysis and H_2S content, while supernatants were used for nitrite/nitrate (NOx) assay.

Table 1
Evaluation of body weight and glycemia in db/db mice.

	WT					db/db				
weeks of age	6	7	8	9	10	6	7	8	9	10
BODY WEIGHT (g)	17,7 ± 0,8 (n=8)	21,6 ± 0,5 (n=8)	20,2 ± 0,4 (n=8)	21,4 ± 0,3 (n=8)	21,5 ± 0,5 (n=8)	26,5 ± 0,8 *** (n=8)	33,7 ± 1,5 *** (n=8)	36,0 ± 0,6 *** (n=8)	36,1 ± 1,7 *** (n=8)	41,0 ± 0,6 *** (n=8)
GLYCEMIA (mg/dl)	168,5 ± 6,5 (n=8)	175,6 ± 9,2 (n=8)	155,9 ± 7,1 (n=8)	153,6 ± 13 (n=8)	167,0 ± 7,3 (n=8)	198,7 ± 25,0 (n=8)	247,4 ± 29,6 (n=8)	487,6 ± 26,2 *** (n=8)	443,6 ± 62,2 *** (n=8)	480,0 ± 58,3 *** (n=8)

Body weight and glycemia were assessed in db/db and WT mice weekly starting from 6 to 10 weeks of age. Values were expressed as mean values ± SEM of n=8 for each group. Statistical analysis was performed by using two-way ANOVA followed by Bonferroni's for multiple comparisons. ***p<0.001 vs. WT

2.3.2. soluble Guanylyl Cyclase ($sGC_{\alpha1\beta1}$) overexpressing cells

Chinase Hamster Ovary (CHO) cells overexpressing subunit α1β1 of sGC were furnished by Bayer, Leverkusen, Germany. Cells were cultured and grown in DMEM/F12 (HAM) supplemented with 2 mmol/L glutamine, 10% heat-inactivated fetal bovine serum, 1 mM sodium pyruvate, 0.9 mM sodium bicarbonate, 50 U/ml penicillin/streptomycin, 2.5 μg/ml Amphotericin B, 1 mg/ml genetic, 0.25 mg/ml zeocin [17]. Cells were incubated for 2 hours with Erucin 1 μM and then collected for persulfidation assay.

2.3.3. Sodium palmitate (SP) preparation

Sodium Palmitate (SP; cat. n. P9767; Merck, Milan, Italy) was conjugated to free fatty acid bovine serum albumin (BSA; cat. n. 126575 EMD Millipore; Darmstadt, Germany) in a molar concentration of 6:1 before use by dissolving in 150 mM NaCl solution. The conjugate solution was mixed by stirring at 37°C for 1 hour until the conjugate solution became clear and pH was adjusted to 7.4. The palmitate-BSA stock was filtered using a 0.22 μm low-protein binding filter (Millipore, Billerica, MA, USA).

2.4. Protein extraction and Western blot analysis

Cells and tissues were homogenized in RIPA buffer according to published procedures [18,19]. 40 μg of proteins were loaded on 8–10% SDS polyacrylamide gels and transferred to PVDF membranes. Then the membranes were incubated overnight at 4 ∘C with the following primary antibodies: mouse monoclonal anti-eNOS (1:1000, BD Biosciences, Milan, Italy), mouse monoclonal anti-CSE (CSE, 1:500, Proteintech; Manchester, UK), rabbit polyclonal anti-CBS (1:1000, Proteintech, Manchester, UK), rabbit polyclonal anti-Caveolin-1 (Cav-1; 1: 1000; Elab Science; Houston, Texas, USA) rabbit polyclonal anti-3MST (1:1000, Novus Biological, USA), rabbit polyclonal anti-PDE5A (1:1000, ElabScience; Houston, Texas, USA), rabbit polyclonal anti-soluble guanylyl cyclase α1 ($sGC_{\alpha1}$ 1:1000, Merck, Milan, Italy), rabbit polyclonal anti-SQRLD (1:1000, Proteintech; Manchester, UK), rabbit polyclonal anti-ETHE-1 (1:1000, Invitrogen; Waltham, Massachusetts, USA)and mouse monoclonal anti-β-actin (1:3000, Merck, Milan, Italy). Images for western blot were obtained by using Chemidoc System (Bio-Rad, Milan, Italy). Band intensity was analyzed by using ImageJ software and optical density (arbitrary units) was reported.

2.5. H_2S assay

H_2S determination was performed using methylene blue-based assay according to published procedures [20,21].

2.6. NOx assay

Assessment of NOx levels was performed according to Vellecco and collagues [22,23]. Briefly, cellular supernatants (120 μL) were incubated with cadmium (50 mg/well) in a microplate for 1 hour to convert NO into NO^{2-}. After centrifugation, total NOx content was determined using a fluorometric method and calculated against a standard curve of sodium nitrite (50–2000 nM).

2.7. Intracellular ROS Measurement

The generation of ROS was evaluated using the fluorescence probe 2′,7′-dichlorofluorescein-diacetate (H_2DCF-DA; Merck cat n. D6883). BAEC (1×10^4cells/well) were plated in 96-multiwell black plates (Corning, USA). At the end of the previously described treatments, cells were incubated with H_2DCF-DA (10 μM) for 30 minutes at 37 °C. Fluorescence (excitation 485 nm, emission 538 nm) was measured using a microplate reader (GloMax®-Multi Detection System, Promega; Madison, WI, USA). The intracellular ROS levels were expressed as relative fluorescence intensity (RFI).

2.8. cGMP determination

Aorta obtained from WT, db/db mice treated or not with Erucin were homogenized in 8 volumes of buffer containing 5% trichloroacetic acid per gram of tissue. Cells overexpressing $sGC_{\alpha1\beta1}$ treated or not with Erucin were lysed in 200 μl of PBS containing 10 μl of 3.3 M HCl according to d'Emmanuele di Villa Bianca and colleagues [24]. cGMP was extracted and measured using a commercially available enzyme immunoassay kit (Cayman Chemical, Michigan, USA) following the manufacturer's instructions [25,26].

2.9. Persulfidation assay

Persulfidation was detected using a modified biotin switch assay as described previously [7,27]. Briefly, sGC overexpressed CHO cells were precipitated with 20% trichloroacetic acid and then washed with 10% and 5% trichloroacetic acid. Following centrifugation, the pellets were resuspended in HENS buffer containing methanethiosulfonate (20 mM). Acetone precipitation was performed, then the pellets obtained were resuspended in lysis buffer containing 50-mM iodoacetyl–PEG2–biotin, and 2.5-mM dimedone, and then incubated for 2 hr at room temperature in the dark. Lysates (500 μg) were precipitated and resuspended in 50-μl Tris–HCl (50 mM, pH 8.5) containing guanidinium chloride (GdmCl 6 mM), and incubated at 95°C for 5 min. A negative control was generated for each sample by adding DTT (1 mM) during biotin cross-linking. 10% of the sample was immediately boiled at 95°C and used for the identification of the levels of $sGC_{\alpha1}$ among the samples (input). 90% of the samples were used for biotin immunoprecipitation overnight (4°C) using a high-capacity streptavidin resin. Persulfidated proteins were detected by SDS-PAGE and Western blotting with a specific antibody against $sGC_{\alpha1}$.

2.10. Data Analysis

All data were reported as mean ± SEM and the number of the replicated experiments for all data sets is at least n=3 except for the *ex vivo* experiments where n=5. The relaxation data were reported as % of relaxation calculated against the maximal contraction to PE-induced tone. Statistical analysis was performed by using one-way or two-way analysis of variance (ANOVA) where appropriate, followed by the Bonferroni or Dunnett posthoc test, where applicable. Data were analyzed by using Prism Graphpad 8.0. Data sets were considered statistically significant when a value of $p < 0.05$ was reached.

3. Results

3.1. CSE/H_2S pathway is defective in BAEC exposed to high concentrations of both sodium palmitate and glucose (SP+HG)

Firstly, we have assessed if, in our in vitro model of BAEC exposed to hyperlipidemic and hyperglycemic conditions, endothelial dysfunction occurs. As shown in Fig. 1A, NOx content, an indirect index of eNOS/NO pathway activation, was significantly reduced in SP+HG-exposed BAEC compared to cells placed in normal conditions (Fig. 1 A). This reduction was coupled to an increase in ROS levels (Fig. 1 B) confirming that, in our experimental setting, endothelial dysfunction takes place. Starting from these findings, we have then assessed the involvement of the H_2S pathway by measuring H_2S levels and the H_2S-generating enzymes expression in SP+HG-exposed BAEC. As shown in Fig. 1C, in cell lysate of BAEC exposed to an SP+HG environment, lower levels of H_2S were detected, when compared to a normal environment. In detail, the basal production of H_2S in cells undergoing SP + HG treatment was not significantly different from cells exposed to vehicle, even though showed an overt trend of reduction. However, when we performed the same measurement, following the addition of L-cysteine, the endogenous substrate for H_2S biosynthesis, we observed a significant increase

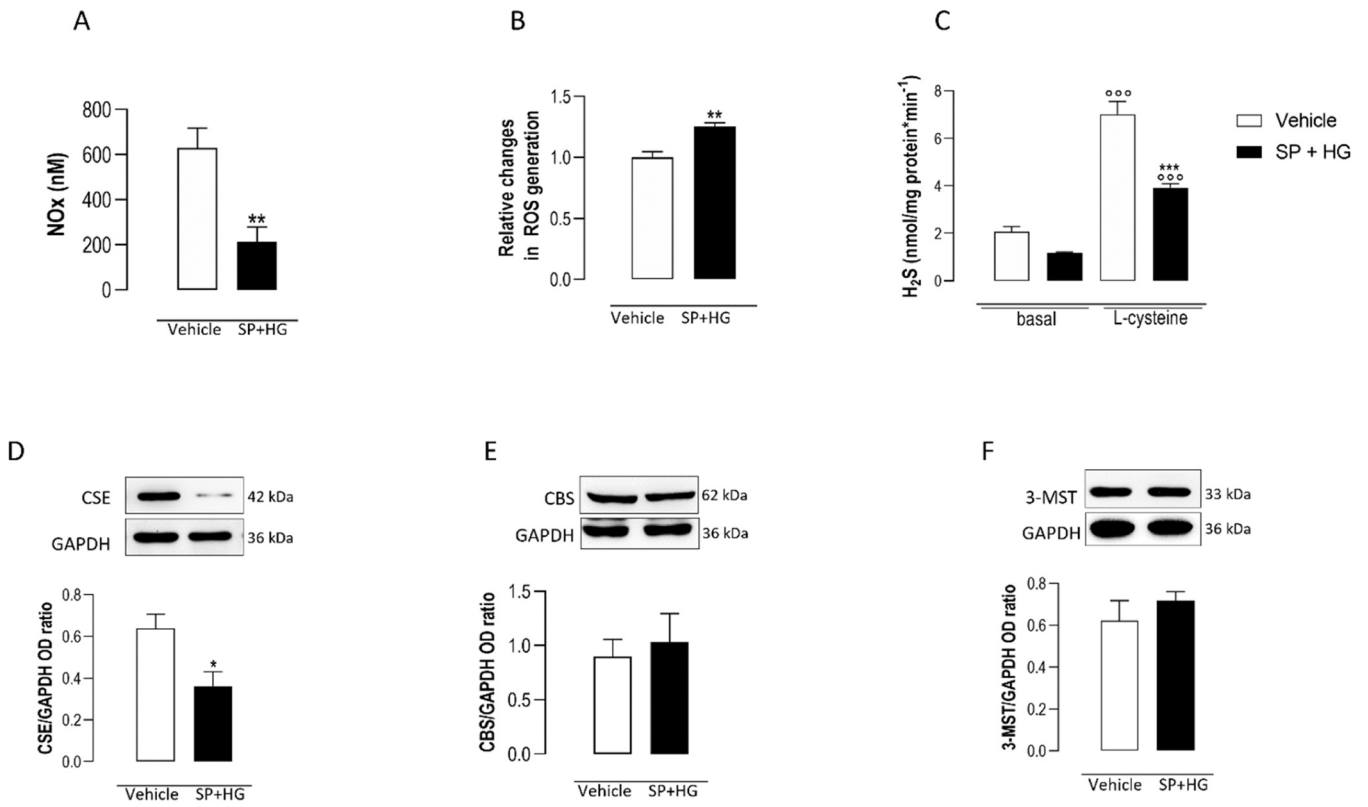

Fig. 1. Evaluation of CSE/H_2S pathway in BAEC exposed to high concentrations of both sodium palmitate and glucose (SP+HG). (A) concentration of total NO levels (expressed as total nitrate/nitrite, NOx) in BAEC exposed to SP+ HG (100 μM and 50 mM, respectively) environment (3 h) or vehicle (BSA/NaCl) and then stimulated with insulin (100 nM; 15 min). Data were expressed as mean ± SEM of n=4 for each group. Statistical analysis was conducted by using Student's T-test, **p < 0.01 vs vehicle. (B) Concentration of intracellular ROS levels in BAEC exposed to SP+HG environment or vehicle and then stimulated with insulin. Data were expressed as fold change compared to the levels of ROS detected in the vehicle, taken as 1 (n= 4). Statistical analysis was conducted by using Student's T-test **p<0.01 vs. vehicle. (C) Levels of H_2S in the total cell lysate of BAEC exposed to SP+HG environment or vehicle and then stimulated with insulin. Data were expressed as mean ± SEM of n=3 for each group. Statistical analysis was conducted by using one-way ANOVA followed by Bonferonni's for multiple comparisons, °°°p < 0.01 vs. own basal; ***p < 0.01 vs. vehicle. (D-F) Representative western blots of at least three separate experiments with similar results. Quantification of CSE (D), CBS (E) and 3-MST (F) protein levels in cell lysates of BAEC exposed to SP+HG environment or vehicle, and then stimulated with insulin. Data were normalized to GAPDH. Values were presented as mean ± SEM. Statistical analysis was conducted by using Student's T-test. *p < 0.05 vs vehicle.

in both vehicle and SP+HG-exposed BAEC, whereas the H_2S production was significantly reduced in SP+HG exposed BAEC compared to the vehicle. In line with the attenuated H_2S content, a reduction in the expression of CSE was detected in SP+HG exposed BAEC (Fig. 1D). Conversely, no change in both CBS and 3-MST expression (the other two H2S-producing enzymes) was observed, in both experimental groups (Fig. 1E-F).

3.2. L-cys/CSE pathway is disrupted in db/db mice contributing to vascular dysfunction coupled to MetS

To verify if the MetS-associated vascular dysfunction could involves a defective CSE/H_2S pathway, we carried out *ex vivo* and molecular experiments on aorta harvested from db/db mice at 10 weeks of age. Firstly, a concentration–response curve to L-cys on Phenilephrine (PE)-stable tone was performed. As shown in Fig. 2A, the vasorelaxation induced by L-Cys was strongly impaired in db/db isolated aorta rings in comparison with WT. A dysregulation in the expression of the H_2S-generating enzymes was also found in db/db mice. Indeed, CSE and CBS expression were significantly lower (Fig. 2B-C), meanwhile 3-MST expression was robustly increased compared to the WT (Fig. 2D). The degrading H_2S enzymes expression was also evaluated, as shown in suppl Fig. 1A-B, and no significant change of ethylmalonic encephalopathy 1 protein (ETHE1), and sulfide quinone reductase (SQRLD), was observed (supplemental Fig. 1A-B). Taken together these results indicate that in MetS-associated vascular dysfunction, there is an altered pattern of expression of H_2S-generating enzymes characterized by a significant impairment of L-cys/CSE/H_2S pathway. To assess whether the impairment of endogenous H_2S production was coupled to a reduced activity of downstream signaling, we evaluated the acute relaxing effect of H_2S-donors, i.e., NaHS and Erucin, on PE-precontracted aortic rings harvested from db/db and WT mice (Fig. 2E-F). Interestingly both NaHS and Erucin concentration-response curves were markedly impaired in aorta harvested from db/db mice indicating an alteration in the downstream pathways activated by H_2S, essential for the vascular function.

3.3. Erucin ameliorates vascular dysfunction in db/db mice independently from eNOS/NO signaling

Since L-cysteine/CSE/H_2S pathway is impaired in db/db mice, the next step was to evaluate if the chronic supplementation of H_2S could improve the vascular impairment observed. Therefore db/db mice were treated orally with Erucin, a slow natural H_2S donor, for 4 weeks (from 6 weeks of age up to 10 weeks of age). In aorta rings harvested following Erucin treatment (3 mg/kg), acetylcholine (Ach)-induced vasorelaxation was significantly improved (Fig. 3A). In contrast, Erucin treatment slightly affected the relaxation induced by β_2 adrenergic agonist Isoprenaline (Fig. 3B). It is well known that the integrity of the endothelium is mandatory for Ach-induced vasodilatation, and it is mainly due to NO release [6]. Differently, Isoprenaline-induced vasorelaxation relies on a double mechanism that involves mainly the β_2 adrenergic receptor activation and to a lesser extent, eNOS/NO/sGC

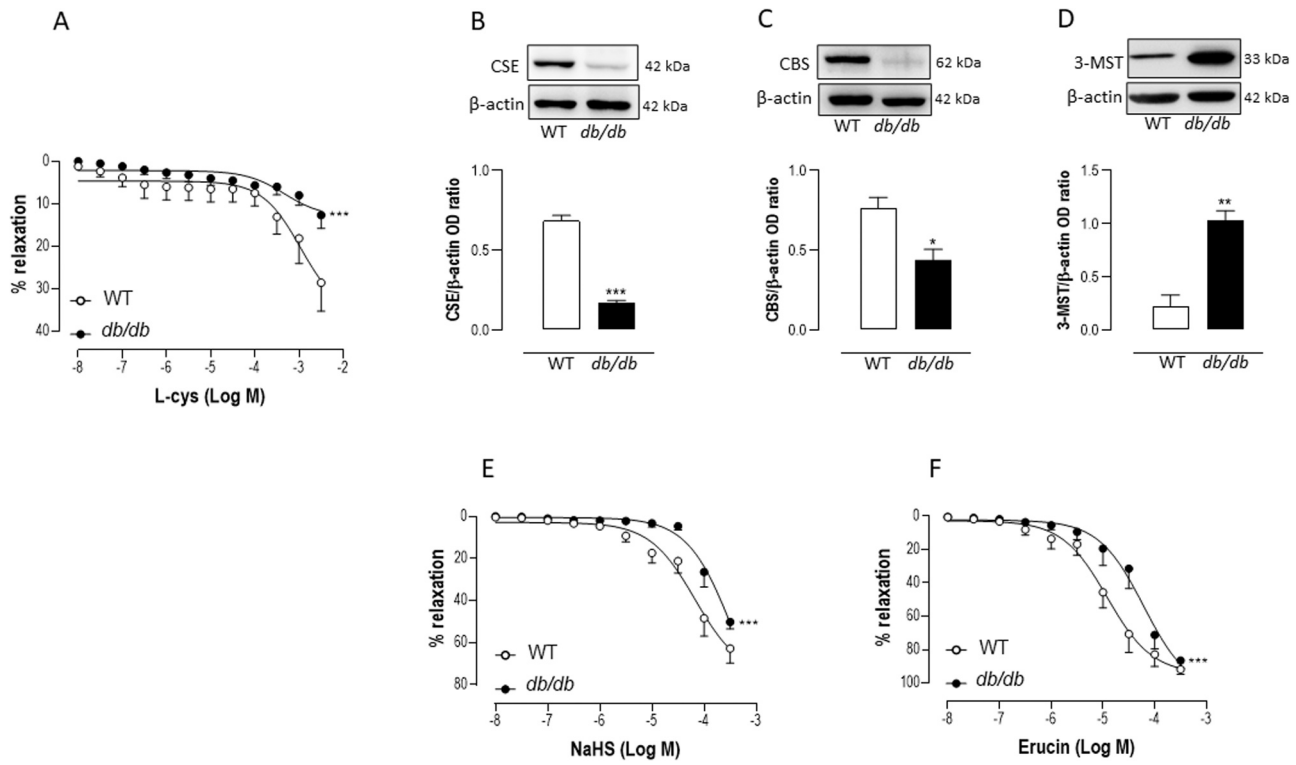

Fig. 2. Evaluation of H_2S signaling in isolated aortic rings of db/db mice. (A) Concentration-response curve of L-cysteine (10 nM-3 mM)- on a stable tone of phenylephrine (PE 1 μM) in aorta rings harvested from db/db and WT mice at 10 weeks of age. Values were expressed as mean values ± SEM of n=6 for each group and expressed as % relaxation. Statistical analysis was performed by using two-way ANOVA followed by Bonferroni's for multiple comparisons. ***p<0.001 vs. WT. **(B-D)** Representative western blots of three separate experiments with similar results. Quantification of CSE **(B)**, CBS **(C)** and 3-MST **(D)** protein levels in aorta lysates of db/db and WT mice at 10 weeks of age. Data were normalized to β-actin. Values were presented as mean ± SEM Statistical analysis was performed by using Student's T-test***p<0.001 vs. WT mice. **(E-F)** Concentration-response curves of NaHS (**E**, 10 nM- 300 **μ**M) and **E**rucin (**F**, 10 nM- 300 μM) on a stable tone of PE in aorta rings harvested from db/db and WT mice at 10 weeks of age. Values were expressed as mean ± SEM of n=5 for each group and expressed as % relaxation. Statistical analysis was performed by using two-way ANOVA followed by Bonferroni's for multiple comparisons. ***p<0.001 vs. WT.

signaling [21]. The finding that Erucin fails to modify Iso-induced vasorelaxation suggests that β_2 activated signal transduction is not involved in Erucin beneficial effect, ruling out cAMP-induced downstream signaling. Therefore, most likely, Erucin displays a targeted action on eNOS/NO/sGC /cGMP pathway. To better dissect if the protective action of Erucin was coupled with eNOS activation, experiments with L-NIO, a selective eNOS inhibitor, were performed. In particular, the increased tension induced by L-NIO administration over a stable tone of PE was evaluated [16,28]. As expected, such treatment resulted in a minor increase in tension in db/db mice compared to WT indicating a reduced NO basal production in these mice (Fig. 3C) and confirming that a defective eNOS function occurs in MetS, as already demonstrated [29]. To further investigate the involvement of eNOS/NO signaling in vascular impairment observed in db/db mice, eNOS and caveolin-1 expression were measured. Caveolin-1 is a membrane resident protein that negatively regulates eNOS activity [30]. As shown in Fig. 3D, eNOS expression was similar among the experimental groups, whilst Cav-1 was significantly augmented in the aorta of db/db mice (Fig. 3E) confirming a reduced activity of eNOS in this strain, in agreement with previous studies [31,32]. Interestingly, as shown in Fig. 3C-E, Erucin treatment did not affect either the L-NIO-induced increase in tension or Cav-1 expression. Taken together, these data strongly suggest that the beneficial effect exerted by Erucin is not due to a direct action on eNOS expression/activity but rather downstream on the NO/sGC/cGMP axis.

3.4. sGC/cGMP axis is dysregulated in db/db mice and Erucin improves vascular impairment via sGC persulfidation

It is well known that NO exerts its vasodilating properties enhancing cGMP synthesis through the activation of soluble guanylyl cyclase (sGC) [2]. As a second messenger, cGMP activates downstream signaling inducing vasorelaxation. The signaling is switched off by the action of phosphodiesterase-5 (PDE5), the main isoform expressed within the vasculature, which selectively hydrolyzes cGMP in the inactive metabolite 5'-GMP [5,6]. To evaluate if the impaired vasorelaxation observed in db/db mice could involve sGC/cGMP signaling, and if Erucin could act on it, the expression of sGC subunit α1 ($sGC_{\alpha1}$), the most abundant subunit within the vasculature, [16,21] and PDE5 were assessed. As shown in Fig. 4A, $sGC_{\alpha1}$ expression was significantly reduced in the aorta of db/db mice in comparison to WT. Conversely, the PDE5 expression did not change among the strains (Fig. 4B). The reduction of cGMP content, measured in the aorta of db/db mice, further corroborates our hypothesis of a reduced expression of sGC in the aorta of these mice (Fig. 4C). These results indicate a defective sGC/cGMP signaling in db/db mice leading to a reduction of the vasorelaxation. As observed for eNOS expression, Erucin treatment did not modify either $sGC_{\alpha1}$ or PDE5 expression (Fig. 4A-B). However, the cGMP content was significantly enhanced by Erucin treatment (Fig. 4C). This finding strongly suggests that Erucin's beneficial action most likely relies on a post-translation modification on sGC, positively modulating its activity. Current evidence, also from our research group, has demonstrated that persulfidation is a new H_2S molecular mechanism of action modifying their biological activity [27,33,34]. To test our hypothesis, by using the dimedone switch method, we explored whether Erucin could persulfidate $sGC_{\alpha1}$ leading to changes in cGMP levels. To do so, we used sGC overexpressed CHO cells. As shown in Fig. 4D, the persulfidation analysis clearly showed that $sGC_{\alpha1}$ was persulfidated in Erucin-treated cells compared to cells exposed to vehicle. Notably, in the presence of a

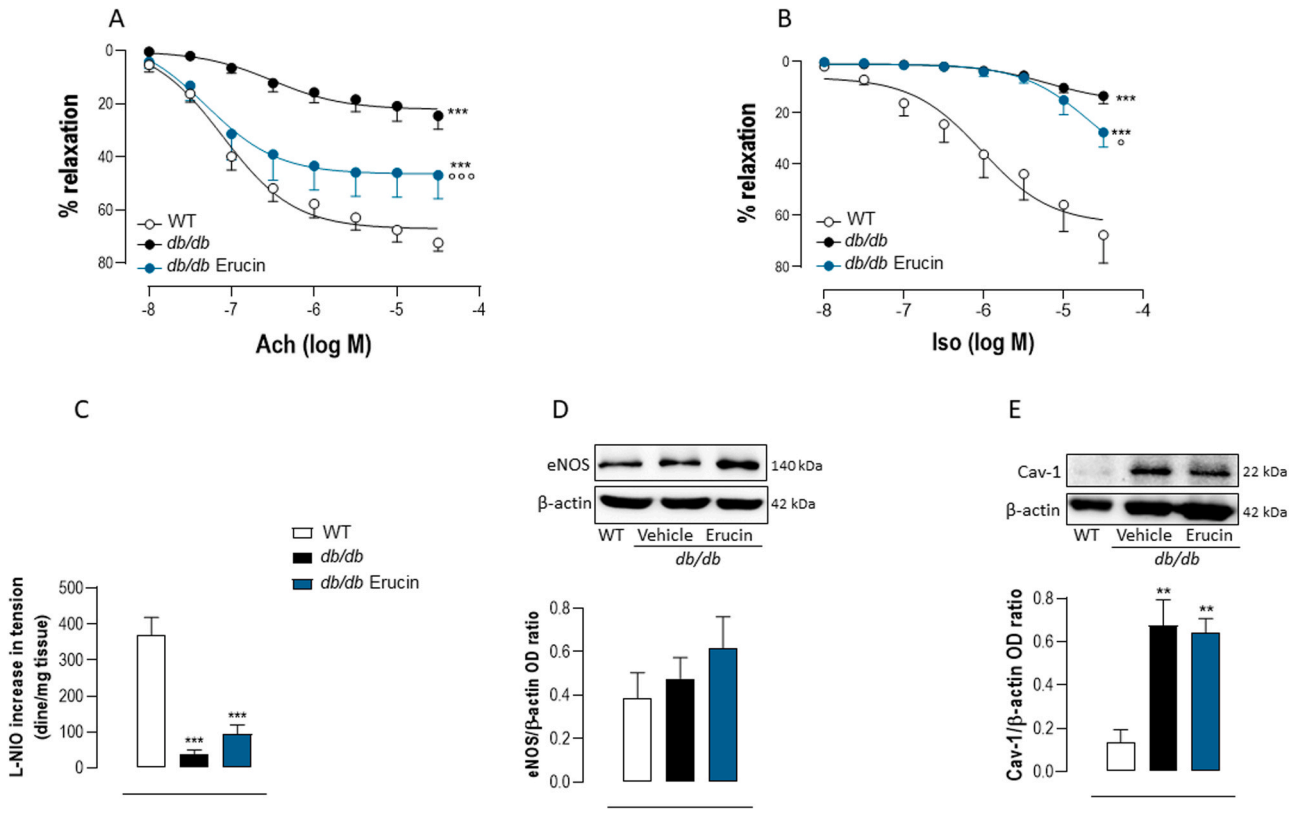

Fig. 3. Effect of Erucin on eNOS/NO pathway in isolated vessels harvested from db/db mice. (A-B) Concentration-response curves of Acetylcholine (A, 10 nM-30μM) and Isoprenaline (B, 10 nM-30μM) on a stable tone of PE (1 μM) in aorta rings harvested from db/db treated or not with Erucin and WT mice at 10 weeks of age. Values were expressed as mean ± SEM of n=5–6 for each group and expressed as % relaxation. Statistical analysis was performed by using two-way ANOVA followed by Bonferroni's for multiple comparisons. ***p<0.001 vs. WT mice, °p<0.05; °°°p<0.001 vs. db/db mice treated with vehicle. **(C)** Increase in tension induced by the exposure of PE-pre-contracted aortic rings (300 nM) to L-NIO (10 μM, 20 min) in aorta rings harvested from db/db treated or not with Erucin and WT mice at 10 weeks of age. Values were expressed as mean ± SEM of n=6 for each group and expressed as dine/mg of tissue. Statistical analysis was performed by using one-way ANOVA followed by Dunnett's for multiple comparisons. ***p<0.001vs. WT mice. **(D-E)** Representative western blots of at least three separate experiments with similar results. Quantification of eNOS **(D)** and Cav-1 **(E)** protein levels in aorta lysates of db/db treated or not with Erucin and WT mice at 10 weeks of age. Data were normalized to β-actin. Values were presented as mean ± SEM. Statistical analysis was performed by using one-way ANOVA followed by Dunnett's for multiple comparisons **p<0.01 vs. WT mice.

reducing agent DTT, the band was reduced, confirming that the detected signal is specific to persulfidation. This data well fit with the cGMP content measured in these cells treated with Erucin. Indeed, as shown in Fig. 4E, the Erucin treatment significantly increased the cGMP levels compared to the vehicle. Taken together, these results demonstrate that: i) in db/db mice associated vascular dysfunction, sGC/cGMP signalling is defective; ii) Erucin, by persulfidating $sGC_{\alpha 1}$, positively modulates sGC activity ameliorating vascular impairment.

4. Discussion

In this study, by using *in vitro* and *ex vivo* approaches, we have shown that in MetS-associated vascular complications, an impairment of TSP takes place with a consequent reduction in H_2S biosynthesis. The reduction of H_2S production is counterbalanced *in vivo* by the supplementation of exogenous H_2S with Erucin, one of the major components of leaves of *Eruca sativa,* a rocket plant belonging to the Brassicaceae family [35].

The *in vitro* data were obtained by setting up an *in vitro* model of MetS. Exposure of BAEC to high concentrations of both sodium palmitate (SP) and glucose (HG), was used to mimic the hyperlipidemic and hyperglycemic conditions occurred in MetS. In this experimental setting, a significant reduction of NOx, coupled with an increase in ROS generation, was found. Thus, this cellular model of MetS, displays both hallmarks of endothelial dysfunction i.e., eNOS/NO signaling impairment, and ROS overproduction [2]. Next, we assessed if the H_2S pathway could be affected in BAEC exposed to the SP+HG environment. The data obtained revealed a reduction of H_2S levels coupled with the down-regulation of CSE expression. This result is in line with our previous reports in which, an impairment of CSE/H_2S pathway, has been demonstrated in vascular inflammation associated with glucocorticoid-induced hypertension, rat spontaneous hypertension (SHR), and in type one diabetes mice models [11,36,37]. Conversely, CBS and 3MST protein expression levels were unchanged confirming the primary role of CSE within vasculature.

To better define the role played by the H_2S pathway in vascular dysfunction associated with MetS, we switched from *in vitro* to *ex vivo* approach by using a well-known genetic mouse model of MetS, i.e., db/db mice. This strain, having a mutation in the gene encoding the leptin receptor ($Lepr^{db}$), is characterized by a deficient leptin signaling which confers susceptibility to obesity, insulin resistance, and type 2 diabetes (T2DM) [38]. Aorta harvested from db/db mice displayed a significant decrease of L-cysteine-induced vasorelaxation associated with a down-regulation of both CBS and CSE expression. This evidence showed similar data obtained from cells, confirming an essential role of H_2S signaling in MetS-induced vascular dysfunction. The finding that the aorta of db/db mice displayed upregulation of the 3MST expression could be most likely due to compensatory mechanisms for rebalancing the physiological H_2S levels. To evaluate if the impairment of H_2S pathway could also involve H_2S-degrading enzymes, the expression of sulfide quinone oxidoreductase (SQRLD) and persulfide dioxygenase (ETHE1) were assessed. The data showed that there was no difference in

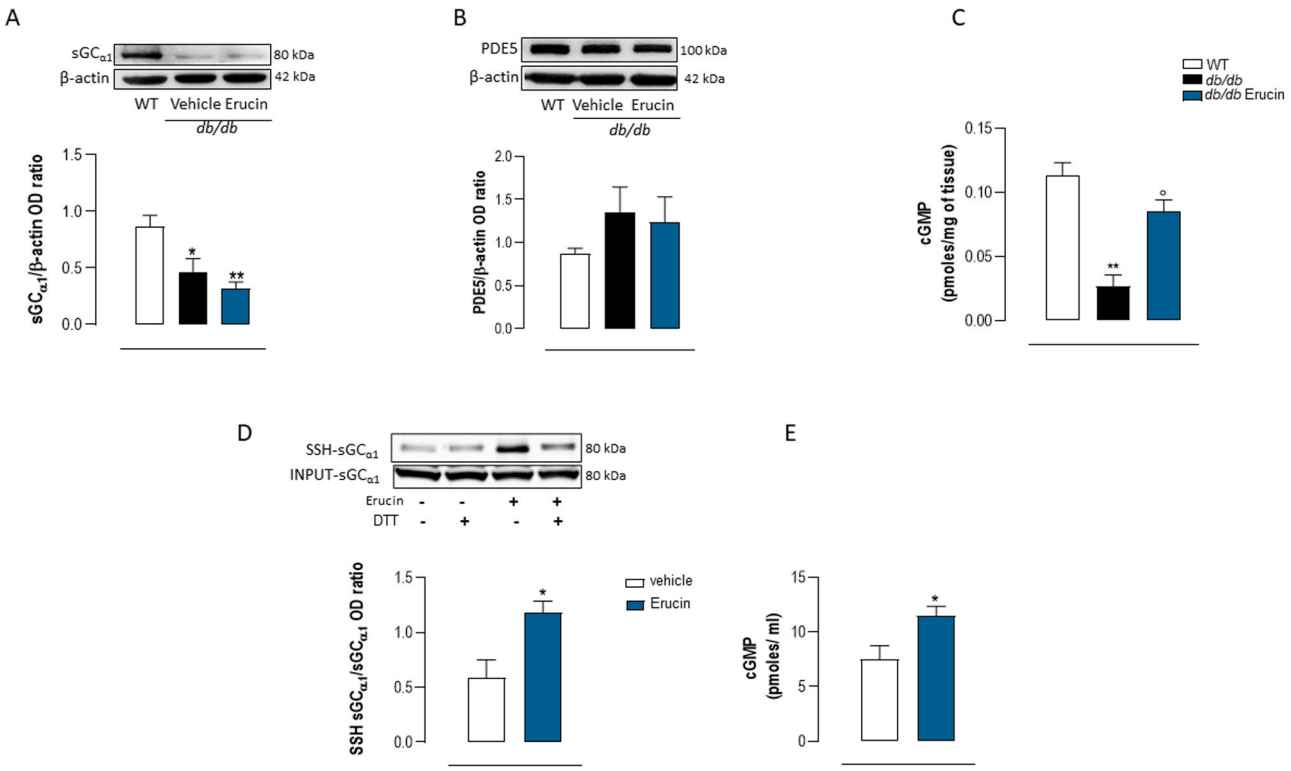

Fig. 4. Effect of Erucin on sGC/cGMP pathway in isolated vessels harvested from db/db mice and in sGC overexpressed CHO cells. (A-B) Representative western blots of at least three separate experiments with similar results. Quantification of $sGC_{\alpha1}$ **(A)** and PDE5 **(B)** protein levels in aorta lysates of db/db treated or not with Erucin and WT mice at 10 weeks of age. Data were normalized to β-actin. Values were presented as mean ± SEM. Statistical analysis was performed by using one-way ANOVA followed by Dunnett's for multiple comparisons **p<0.01 vs. WT mice. (C) cGMP levels in aorta harvested from db/db treated or not with Erucin and WT mice at 10 weeks of age. Values were expressed as mean ± SEM of n=3 for each group and expressed as pmoles/mg of proteins. Statistical analysis was performed by using one-way ANOVA followed by Dunnett's for multiple comparisons ***p<0.001 vs. WT mice, °p<0.05 vs. db/db treated with vehicle(D) Representative western blot of three separate experiments with similar results. Quantification of $sGC_{\alpha1}$ persufidation levels in cell lysates of sGC overexpressed CHO cells treated with Erucin (1 μM; 2 h) or vehicle. DTT, a reducing agent, was used to eliminate the modification prior to detection. Data were expressed as mean values ± SEM. Statistical analysis was performed by using Student's T-test *p<0.05 vs. vehicle. (E) cGMP content in sGC overexpressed CHO cells treated with Erucin or vehicle. Data were expressed as mean ± SEM of n=4 for each group. Statistical analysis was performed by using Student's T-test *p<0.05 vs. vehicle.

both enzymes' expression between wild-type and db/db mice. Taken together, these findings suggest that the impaired CSE-derived H_2S synthesis contributes, together with the augmented ROS generation and the dysregulation of eNOS/NO pathway, to vascular dysfunction observed in MetS.

To further dissect the molecular mechanisms of eNOS/NO signaling impairment, both pharmacological and molecular approaches were applied by using aortas harvested from db/db mice. In the organ bath studies, Ach- and Iso-induced vasorelaxation were evaluated and compared to WT mice. It is known that Ach and Iso effect relies on different signal transduction mechanisms. Indeed, Ach-induced vasorelaxation is mediated by eNOS-derived NO [39], whilst Iso-induced vasorelaxation involves β_2 adrenergic G_s coupled protein activation, with raised levels of cAMP and, to a lesser extent, eNOS/NO/sGC signaling [40,41]. In db/db mice both Ach- and Iso-induced vasorelaxation are strongly impaired. Interestingly, Erucin treatment exclusively improved Ach-induced vasorelaxation, causing over 50% amelioration of the E_{max}. The finding that Erucin fails to modulate the Iso-induced vasorelaxation suggests that β_2 activated signal transduction is not involved in Erucin beneficial effect, ruling out cAMP-induced signaling. To further assess a role of eNOS/NO/sGC pathway in the beneficial effect of Erucin, evaluation of eNOS and Cav-1 expression was performed. Western blot analysis revealed an altered expression of eNOS/Cav-1 ratio in db/db mice. Indeed, a significant increase of Cav-1, but not of eNOS, expression was observed. Taken together, these findings indicate that in db/db mice a defective eNOS/NO signaling occurs. Specifically, the increased Cav-1 expression keeps eNOS in a less active state with consequent reduced NO production [31]. Interestingly, Erucin treatment did not modify either eNOS or Cav-1 expression suggesting that Erucin beneficial effect on vasculature does not involve eNOS function. This evidence is corroborated by L-NIO experiments in isolated organ bath. Indeed, the minor increase in tension observed in db/db mice following L-NIO exposure, compared to WT mice, further indicates that in db/db mice a defective eNOS/NO signaling occurred due to Cav-1 overexpression. Notably, Erucin treatment did not modify L-NIO increased tension compared to vehicle, strengthening our hypothesis of NO/sGC/cGMP signaling involvement in Erucin beneficial effect, ruling out eNOS.

The NO signaling starts from the endothelium leading to activation of sGC in smooth muscle cells. Endothelium-derived NO permeates through the vascular smooth muscle cells where binds sGC, promoting cGMP production that, in turn, activates a downstream signaling which culminates in vasodilatation [2]. The cGMP signaling is turned off by the action of phosphodiesterase-5 (PDE)-5, the main isoform expressed within the vasculature, which selectively hydrolyses cGMP in its inactive metabolite 5'-GMP [5]. Moreover, it is well established that H_2S is an endogenous inhibitor of PDEs activity, preserving cGMP catabolism [5,6]. In db/db mice aorta cGMP levels were almost 4-fold reduced as compared to WT and this effect could be attributable to i) an increased cGMP degradation due to an enhanced expression/activity of PDE-5; ii) a diminished cGMP production caused by a reduced expression/activity of sGC. Therefore, we determined the expression of PDE5 and sGC subunit α1 (the most abundant subunit within the vasculature, [16,21]) in aorta harvested from both strains finding a significant reduced

expression of $sGC_{\alpha1}$ in db/db mice vessels only. Conversely, PDE5 expression was unchanged, implying that in MetS-associated vascular complications, the reduced levels of cGMP were mainly due to a defective sGC/cGMP signalling. It is important to stress that low levels of cGMP are even worsted by the increased activity of PDE5, due to the reduced endogenous levels of H_2S [5,6]. Thus, in db/db mice L-cys/CSE pathway disruption leads to a reduced level of cGMP levels that are not only due to a diminished sGC expression, but also to an enhanced cGMP degradation operated by PDE5, in absence of H_2S negative regulation. The involvement of this molecular mechanism in vascular dysfunction is further supported by the in vitro data obtained from db/db mice aorta. Vasorelaxation induced by H_2S donors in PE-precontracted aortic rings shows a significant reduction of vasodilating concentration-response curves to NaHS and/or Erucin, compared to WT. This finding demonstrates that despite the acute inhibition of PDE operated by the administration of H2S donors, we still observed an impaired vasorelaxation, most likely due to a low cGMP- derived sGC content. For this reason, we determined the effect exerted by chronic administration of Erucin on sGC/cGMP axis.

Interestingly, in aorta of db/db mice the treatment with Erucin did not modify the PDE5 and $sGC_{\alpha1}$ expressions, nevertheless it fully recovered the cGMP content. Most likely, chronic administration of Erucin, by releasing H_2S, put PDE5 in a reduced activity state, enhancing cGMP content. An additive explanation for the full recovery of cGMP levels could be due to a direct action of H_2S on sGC activity. Indeed, it has been shown that H_2S can influence the redox state of sGC and thus its activity [42,43]. However, the molecular mechanism through which H_2S can modulate sGC activity is not yet clarified. Persulfidation is a recent discovered biological effect elicited by H_2S. Specifically, it is a post-translational modification (PTM) of proteins on L-cysteine residue that modifies protein biological activity [33,44–46]. By using overexpressed sGC cells, we demonstrated that Erucin persulfidated $sGC_{\alpha1}$ and this event was coupled with an increase in cGMP levels. This evidence suggests that Erucin-derived H_2S can modify sGC activity, through the PTM persulfidation, leading to an enhanced enzymatic activity, detectable as an increase of cGMP content.

It should be considered that cGMP increased levels could be also due to an additional mechanism. Indeed, recently it has been demonstrated that low levels of NO keep NO/sGC pathway more active [47].

In summary, we showed that in db/db mice the vascular dysfunction coupled with MetS is characterized by an impairment of L-cys/CSE/H_2S/PDE/cGMP and eNOS/NO/sGC/cGMP pathways, both converging on a reduced level of cGMP (see graphical abstract). Erucin treatment, by releasing H_2S, improves vascular dysfunction through two complementary actions: i) the direct interaction with sGC via persulfidation; ii) the inhibitory effect on PDE activity, both mechanisms leading to an enhancement of cGMP levels.

5. Conclusions

Our study demonstrated that in db/db mice, the reduced level of cGMP is the main hallmark of impaired vasorelaxation. This feature is due to the damaging of both H_2S and NO signaling. The exogenous H_2S supplementation, through the H_2S donor Erucin, by acting on smooth muscle component of the vessels, i.e. upstream on sGC and downstream on PDE5, fosters cGMP content, ameliorating vascular function.

Hence, by taking advantage from Erucin, our study suggests a potential use of natural H_2S donors, as a promising alternative/additive approach, in the complex management of MetS therapy and supports the importance of a correct lifestyle and nutrition in MetS patients.

Funding

This work was supported by Ministero dell'Università e della Ricerca (MUR)—PRIN 2022 n. 202275M25F "Finanziato dall'Unione europea – Next Generation EU".

Declaration of Competing Interest

The authors declare no conflict of interest.

Appendix A. Supporting information

Supplementary data associated with this article can be found in the online version at doi:10.1016/j.biopha.2024.116466.

References

[1] D. Ambroselli, F. Masciulli, E. Romano, G. Catanzaro, Z.M. Besharat, M.C. Massari, E. Ferretti, S. Migliaccio, L. Izzo, A. Ritieni, et al., New advances in metabolic syndrome, from prevention to treatment: the role of diet and food, Nutrients *15* (2023) 640, https://doi.org/10.3390/nu15030640.
[2] G. Cirino, V. Vellecco, M. Bucci, Nitric oxide and hydrogen sulfide: the gasotransmitter paradigm of the vascular system, Br. J. Pharmacol. *174* (2017) 4021–4031, https://doi.org/10.1111/bph.13815.
[3] G. Cirino, C. Szabo, A. Papapetropoulos, Physiological roles of hydrogen sulfide in mammalian cells, tissues, and organs, Physiol. Rev. *103* (2023) 31–276, https://doi.org/10.1152/physrev.00028.2021.
[4] V. Vellecco, C. Armogida, M. Bucci, Hydrogen sulfide pathway and skeletal muscle: an introductory review, Br. J. Pharmacol. *175* (2018) 3090–3099, https://doi.org/10.1111/bph.14358.
[5] M. Bucci, A. Papapetropoulos, V. Vellecco, Z. Zhou, A. Pyriochou, C. Roussos, F. Roviezzo, V. Brancaleone, G. Cirino, Hydrogen sulfide is an endogenous inhibitor of phosphodiesterase activity, Arterioscler. Thromb. Vasc. Biol. *30* (2010) 1998–2004, https://doi.org/10.1161/ATVBAHA.110.209783.
[6] M. Bucci, A. Papapetropoulos, V. Vellecco, Z. Zhou, A. Zaid, P. Giannogonas, A. Cantalupo, S. Dhayade, K.P. Karalis, R. Wang, et al., cGMP-dependent protein kinase contributes to hydrogen sulfide-stimulated vasorelaxation, PLoS One *7* (2012) e53319, https://doi.org/10.1371/journal.pone.0053319.
[7] S.-I. Bibli, J. Hu, F. Sigala, I. Wittig, J. Heidler, S. Zukunft, D.I. Tsilimigras, V. Randriamboavonjy, J. Wittig, B. Kojonazarov, et al., Cystathionine γ Lyase sulfhydrates the RNA binding protein human antigen R to preserve endothelial cell function and delay atherogenesis, Circulation *139* (2019) 101–114, https://doi.org/10.1161/CIRCULATIONAHA.118.034757.
[8] A. Harper, M. Chapel, G. Hodgson, K. Malinowski, I. Yates, M. Garle, V. Ralevic, GYY4137, a hydrogen sulfide donor, protects against endothelial dysfunction in porcine coronary arteries exposed to myeloperoxidase and hypochlorous acid, Vasc. Pharmacol. *152* (2023) 107199, https://doi.org/10.1016/j.vph.2023.107199.
[9] R. Montanaro, V. Vellecco, R. Torregrossa, G.M. Casillo, O.L. Manzo, E. Mitidieri, M. Bucci, S. Castaldo, R. Sorrentino, M. Whiteman, et al., Hydrogen sulfide donor AP123 restores endothelial nitric oxide-dependent vascular function in hyperglycemia via a CREB-dependent pathway, Redox Biol. *62* (2023) 102657, https://doi.org/10.1016/j.redox.2023.102657.
[10] H. Zhao, S. Lu, J. Chai, Y. Zhang, X. Ma, J. Chen, Q. Guan, M. Wan, Y. Liu, Hydrogen sulfide improves diabetic wound healing in Ob/Ob mice via attenuating inflammation, J. Diabetes Complicat. *31* (2017) 1363–1369, https://doi.org/10.1016/j.jdiacomp.2017.06.011.
[11] V. Brancaleone, F. Roviezzo, V. Vellecco, L. De Gruttola, M. Bucci, G. Cirino, Biosynthesis of H2S is impaired in non-obese diabetic (NOD) mice, Br. J. Pharmacol. *155* (2008) 673–680, https://doi.org/10.1038/bjp.2008.296.
[12] N. Liu, M. Li, S. Liu, J. Kang, L. Chen, J. Huang, Y. Wang, H. Chen, W. Zhang, Exogenous H2S attenuates hypertension by regulating renin exocytosis under hyperglycaemic and hyperlipidaemic conditions, Int. J. Mol. Sci. *24* (2023) 1690, https://doi.org/10.3390/ijms24021690.
[13] N. Liu, J. Wu, L. Zhang, Z. Gao, Y. Sun, M. Yu, Y. Zhao, S. Dong, F. Lu, W. Zhang, Hydrogen sulphide modulating mitochondrial morphology to promote mitophagy in endothelial cells under high-glucose and high-palmitate, J. Cell Mol. Med. *21* (2017) 3190–3203, https://doi.org/10.1111/jcmm.13223.
[14] N. Percie du Sert, V. Hurst, A. Ahluwalia, S. Alam, M.T. Avey, M. Baker, W. J. Browne, A. Clark, I.C. Cuthill, U. Dirnagl, et al., The ARRIVE Guidelines 2.0: updated guidelines for reporting animal research, PLoS Biol. *18* (2020) e3000410, https://doi.org/10.1371/journal.pbio.3000410.
[15] V. Vellecco, A. Saviano, F. Raucci, G.M. Casillo, A.A. Mansour, E. Panza, E. Mitidieri, G.D. Femminella, N. Ferrara, G. Cirino, et al., Interleukin-17 (IL-17) triggers systemic inflammation, peripheral vascular dysfunction, and related prothrombotic state in a mouse model of Alzheimer's Disease, Pharmacol. Res. *187* (2023) 106595, https://doi.org/10.1016/j.phrs.2022.106595.
[16] E. Mitidieri, V. Vellecco, V. Brancaleone, D. Vanacore, O.L. Manzo, E. Martin, I. Sharina, Y. Krutsenko, M.C. Monti, E. Morretta, et al., Involvement of 3',5'-cyclic inosine monophosphate in cystathionine γ-lyase-dependent regulation of the vascular tone, Br. J. Pharmacol. *178* (2021) 3765–3782, https://doi.org/10.1111/bph.15516.
[17] F. Wunder, J.-P. Stasch, J. Hütter, C. Alonso-Alija, J. Hüser, E. Lohrmann, A cell-based cGMP assay useful for ultra-high-throughput screening and identification of modulators of the nitric oxide/cGMP pathway, Anal. Biochem. *339* (2005) 104–112, https://doi.org/10.1016/j.ab.2004.12.025.
[18] V. Brancaleone, I. Esposito, A. Gargiulo, V. Vellecco, A. Asimakopoulou, V. Citi, V. Calderone, T. Gobbetti, M. Perretti, A. Papapetropoulos, et al., D-Penicillamine Modulates Hydrogen Sulfide (H2S) Pathway through Selective Inhibition of

Cystathionine-γ-Lyase, Br. J. Pharmacol. *173* (2016) 1556–1565, https://doi.org/10.1111/bph.13459.
[19] E. Panza, I. Bello, M. Smimmo, V. Brancaleone, E. Mitidieri, M. Bucci, G. Cirino, R. Sorrentino, D. Emmanuele di Villa Bianca, R. Endogenous and Exogenous Hydrogen Sulfide Modulates Urothelial Bladder Carcinoma Development in Human Cell Lines, Biomed. Pharm. *151* (2022) 113137, https://doi.org/10.1016/j.biopha.2022.113137.
[20] V. Brancaleone, E. Mitidieri, R.J. Flower, G. Cirino, M. Perretti, Annexin A1 mediates hydrogen sulfide properties in the control of inflammation, J. Pharmacol. Exp. Ther. *351* (2014) 96–104, https://doi.org/10.1124/jpet.114.217034.
[21] V. Vellecco, A. Mancini, A. Ianaro, V. Calderone, C. Attanasio, A. Cantalupo, B. Andria, G. Savoia, E. Panza, A. Di Martino, et al., Cystathionine β-synthase-derived hydrogen sulfide is involved in human malignant hyperthermia, Clin. Sci. (Lond.) *130* (2016) 35–44, https://doi.org/10.1042/CS20150521.
[22] V. Vellecco, E. Esposito, C. Indolfi, A. Saviano, E. Panza, M. Bucci, V. Brancaleone, G. Cirino, R. d'Emmanuele di Villa Bianca, R. Sorrentino, et al., Biphasic Inflammatory Response Induced by Intra-Plantar Injection of L-Cysteine: Role of CBS-Derived H2S and S1P/NO Signaling, Biomed. Pharm. *167* (2023) 115536, https://doi.org/10.1016/j.biopha.2023.115536.
[23] E. Günay, S. Celik, S. Sarinc-Ulasli, A. Özyürek, Ö. Hazman, S. Günay, M. Özdemir, M. Ünlü, Comparison of the anti-inflammatory effects of proanthocyanidin, quercetin, and damnacanthal on benzo(a)pyrene exposed A549 alveolar cell line, Inflammation *39* (2016) 744–751, https://doi.org/10.1007/s10753-015-0301-3.
[24] di Villa Bianca, R. d'Emmanuele, E. Mitidieri, V. Mirone, F. Fusco, C. Imbimbo, G. Cirino, Sorrentino, R. An Ex Vivo Standardized Assay to Measure Human Platelet cGMP, J. Pharmacol. Toxicol. Methods *64* (2011) 164–167, https://doi.org/10.1016/j.vascn.2011.07.001.
[25] V. Mirone, R. d'Emmanuele di Villa Bianca, E. Mitidieri, C. Imbimbo, F. Fusco, P. Verze, D.F. Vitale, R. Sorrentino, G. Cirino, Platelet cyclic guanosine monophosphate as a biomarker of phosphodiesterase type 5 inhibitor efficacy in the treatment of erectile dysfunction: a randomized placebo-controlled study, Eur. Urol. *56* (2009) 1067–1073, https://doi.org/10.1016/j.eururo.2009.09.031.
[26] E. Mitidieri, T. Tramontano, E. Donnarumma, V. Brancaleone, G. Cirino, D. Emmanuele, di Villa Bianca, R.; Sorrentino, R. L-Cys/CSE/H2S Pathway Modulates Mouse Uterus Motility and Sildenafil Effect, Pharmacol. Res. *111* (2016) 283–289, https://doi.org/10.1016/j.phrs.2016.06.017.
[27] V. Vellecco, A. Martelli, I.S. Bibli, M. Vallifuoco, O.L. Manzo, E. Panza, V. Citi, V. Calderone, G. de Dominicis, C. Cozzolino, et al., Anomalous Kv 7 Channel Activity in Human Malignant Hyperthermia Syndrome Unmasks a Key Role for H2 S and Persulfidation in Skeletal Muscle, Br. J. Pharmacol. *177* (2020) 810–823, https://doi.org/10.1111/bph.14700.
[28] A. Katsouda, M. Markou, P. Zampas, A. Varela, C.H. Davos, V. Vellecco, G. Cirino, M. Bucci, A. Papapetropoulos, CTH/MPST double ablation results in enhanced vasorelaxation and reduced blood pressure via upregulation of the eNOS/sGC Pathway, Front. Pharmacol. *14* (2023) 1090654, https://doi.org/10.3389/fphar.2023.1090654.
[29] N.A. Sallam, I. Laher, Redox signaling and regional heterogeneity of endothelial dysfunction in Db/Db Mice, Int. J. Mol. Sci. *21* (2020) 6147, https://doi.org/10.3390/ijms21176147.
[30] M. Bucci, J.P. Gratton, R.D. Rudic, L. Acevedo, F. Roviezzo, G. Cirino, W.C. Sessa, In vivo delivery of the caveolin-1 Scaffolding domain inhibits nitric oxide synthesis and reduces inflammation, Nat. Med. *6* (2000) 1362–1367, https://doi.org/10.1038/82176.
[31] T.Y. Lam, S.W. Seto, Y.M. Lau, L.S. Au, Y.W. Kwan, S.M. Ngai, K.W. Tsui, Impairment of the vascular relaxation and differential expression of caveolin-1 of the aorta of diabetic +db/+db Mice, Eur. J. Pharmacol. *546* (2006) 134–141, https://doi.org/10.1016/j.ejphar.2006.07.003.
[32] M. Bucci, F. Roviezzo, V. Brancaleone, M.I. Lin, A. Di Lorenzo, C. Cicala, A. Pinto, W.C. Sessa, S. Farneti, S. Fiorucci, et al., Diabetic mouse angiopathy is linked to progressive sympathetic receptor deletion coupled to an enhanced caveolin-1 expression, Arterioscler. Thromb. Vasc. Biol. *24* (2004) 721–726, https://doi.org/10.1161/01.ATV.0000122362.44628.09.
[33] V. Vellecco, E. Panza, S.-I. Bibli, G.M. Casillo, F. Raucci, O.L. Manzo, M. Smimmo, R. Villani, M.R. Cavezza, I. Fleming, et al., Phosphodiesterases S-sulfhydration contributes to human skeletal muscle function, Pharmacol. Res. *177* (2022) 106108, https://doi.org/10.1016/j.phrs.2022.106108.
[34] L. Testai, R. Montanaro, L. Flori, E. Pagnotta, V. Vellecco, E. Gorica, L. Ugolini, L. Righetti, V. Brancaleone, M. Bucci, et al., Persulfidation of mitoKv7.4 channels contributes to the cardioprotective effects of the H2S-donor erucin against ischemia/reperfusion injury, Biochem. Pharmacol. *215* (2023) 115728, https://doi.org/10.1016/j.bcp.2023.115728.
[35] A. Martelli, R. d'Emmanuele di Villa Bianca, G. Cirino, R. Sorrentino, V. Calderone, M. Bucci, Hydrogen sulfide and sulfaceutic or sulfanutraceutic agents: classification, differences and relevance in preclinical and clinical studies, Pharmacol. Res. *196* (2023) 106947, https://doi.org/10.1016/j.phrs.2023.106947.
[36] R. d'Emmanuele di Villa Bianca, E. Mitidieri, E. Donnarumma, T. Tramontano, V. Brancaleone, G. Cirino, M. Bucci, R. Sorrentino, Hydrogen sulfide is involved in dexamethasone-induced hypertension in rat, Nitric Oxide *46* (2015) 80–86, https://doi.org/10.1016/j.niox.2014.11.013.
[37] M. Bucci, V. Vellecco, A. Cantalupo, V. Brancaleone, Z. Zhou, S. Evangelista, V. Calderone, A. Papapetropoulos, G. Cirino, Hydrogen sulfide accounts for the peripheral vascular effects of zofenopril independently of ACE inhibition, Cardiovasc. Res. *102* (2014) 138–147, https://doi.org/10.1093/cvr/cvu026.
[38] F. Suriano, S. Vieira-Silva, G. Falony, M. Roumain, A. Paquot, R. Pelicaen, M. Régnier, N.M. Delzenne, J. Raes, G.G. Muccioli, et al., Novel insights into the genetically obese (Ob/Ob) and Diabetic (Db/Db) mice: two sides of the same coin, Microbiome *9* (2021) 147, https://doi.org/10.1186/s40168-021-01097-8.
[39] U. Förstermann, W.C. Sessa, Nitric oxide synthases: regulation and function, 837a–837d, Eur. Heart J. *33* (2012) 829–837, https://doi.org/10.1093/eurheartj/ehr304.
[40] S. Banquet, E. Delannoy, A. Agouni, C. Dessy, S. Lacomme, F. Hubert, V. Richard, B. Muller, V. Leblais, Role of G(i/o)-Src Kinase-PI3K/Akt pathway and caveolin-1 in B_2-adrenoceptor coupling to endothelial NO synthase in mouse pulmonary artery, Cell Signal *23* (2011) 1136–1143, https://doi.org/10.1016/j.cellsig.2011.02.008.
[41] V. Vellecco, E. Mitidieri, A. Gargiulo, V. Brancaleone, D. Matassa, T. Klein, F. Esposito, G. Cirino, M. Bucci, Vascular effects of linagliptin in non-obese diabetic mice are glucose-independent and involve positive modulation of the endothelial Nitric Oxide Synthase (eNOS)/Caveolin-1 (CAV-1) pathway, Diabetes Obes. Metab. *18* (2016) 1236–1243, https://doi.org/10.1111/dom.12750.
[42] Z. Zhou, E. Martin, I. Sharina, I. Esposito, C. Szabo, M. Bucci, G. Cirino, A. Papapetropoulos, Regulation of soluble guanylyl cyclase redox state by hydrogen sulfide, Pharmacol. Res. *111* (2016) 556–562, https://doi.org/10.1016/j.phrs.2016.06.029.
[43] M.A. Olivencia, E. Esposito, V. Brancaleone, S. Castaldo, G. Cirino, F. Pérez-Vizcaino, R. Sorrentino, R. d'Emmanuele di Villa Bianca, E. Mitidieri, Hydrogen sulfide regulates the redox state of soluble guanylate cyclase in CSE-/- mice corpus cavernosum microcirculation, Pharmacol. Res. *194* (2023) 106834, https://doi.org/10.1016/j.phrs.2023.106834.
[44] S.-I. Bibli, I. Fleming, Oxidative post-translational modifications: a focus on cysteine S-sulfhydration and the regulation of endothelial fitness, Antioxid. Redox Signal *35* (2021) 1494–1514, https://doi.org/10.1089/ars.2021.0162.
[45] B.D. Paul, S.H. Snyder, H_2S signalling through protein sulfhydration and beyond, Nat. Rev. Mol. Cell Biol. *13* (2012) 499–507, https://doi.org/10.1038/nrm3391.
[46] B. He, Z. Zhang, Z. Huang, X. Duan, Y. Wang, J. Cao, L. Li, K. He, E.C. Nice, W. He, et al., Protein persulfidation: rewiring the hydrogen sulfide signaling in cell stress response, Biochem Pharmacol. *209* (2023) 115444, https://doi.org/10.1016/j.bcp.2023.115444.
[47] A. Ghosh, M.P. Sumi, B. Tupta, T. Okamoto, K. Aulak, M. Tsutsui, H. Shimokawa, S. C. Erzurum, D.J. Stuehr, Low levels of nitric oxide promotes heme maturation into several hemeproteins and is also therapeutic, Redox Biol. *56* (2022) 102478, https://doi.org/10.1016/j.redox.2022.102478.